Role of Aluminum Salts in the Synthesis of Polymer-Templated Periodic Mesoporous Organosilicas

Eun-Bum Cho,[†] Dukjoon Kim,*[,†] and Mietek Jaroniec*[,‡]

Polymer Technology Institute, Department of Chemical Engineering, Sungkyunkwan University, Suwon, Gyeonggi-do 440–746, Korea, and Department of Chemistry, Kent State University, Kent, Ohio 44242

Received August 15, 2007. Revised Manuscript Received January 20, 2008

The effect of trivalent aluminum salts as well as mono- (KCl) and divalent ($CaCl_2$) salts was investigated in the synthesis of periodic mesoporous organosilicas (PMOs), ethane-silica, and benzene-silica, carried out in the presence of poly(ethylene oxide)-containing nonionic triblock copolymers. Poly(ethylene oxide)-poly(DL-lactic acid-co-glycolic acid)-poly(ethylene oxide) (PEO-PLGA-PEO) triblock copolymer was employed as a soft template and aluminum chloride ($AlCl_3$), sodium aluminate ($NaAlO_2$), and aluminum butoxide ($Al(O^sBt)_3$) were used as auxiliary aluminum compounds. For comparison, analogous PMOs were prepared by using KCl and $CaCl_2$. It was shown that among additives used sodium aluminate had a pronounced effect on the porosity of 2D hexagonal (*p6mm*) ethane-silica mesostructures when adequate Al/ethane molar ratio (about 0.25) was used; namely, the mesopore diameter, BET surface area, and pore volume increased from 8.62 to 9.27 nm, from 897 to 1072 $m^2\ g^{-1}$, and from 1.23 to 1.72 $cm^3\ g^{-1}$, respectively, and the wall thickness decreased from 3.50 to 2.05 nm. Importantly, highly ordered 2D hexagonal benzene-silica mesostructure was formed using $AlCl_3$ (Al/benzene ratio ≥ 1) instead of HCl; such improvement of the structure was not observed for the samples prepared in the presence of other salts, KCl and $CaCl_2$. Also, the crystallinity of benzene-silica mesostructures self-assembled in the presence of aluminum compounds was enhanced.

Introduction

Since the discovery of M41S in 1992,[1] mesoporous silica materials have been developed intensively by using various inorganic precursors and structure directing agents.[2–6] Potential applications of these materials, especially in catalysis, adsorption, and separation-based processes, often require siliceous frameworks with organic functionalities to achieve the desired selectivity.[7–10] Moreover, large uniform and accessible pores as well as macroscopic morphology are crucial factors to achieve the required performance of the aforementioned materials.[11–15] Among numerous efforts to improve properties of mesoporous materials, periodic mesoporous organosilicas (PMOs) prepared by co-condensation of organo-bridged silsesquioxane precursors in the presence of surfactant templates have attracted a lot of attention because of tremendous opportunities to tune the surface, structural, optical, mechanical, and hydrothermal properties of these materials.[16–21]

One of the significant accomplishments in the area of PMOs was the synthesis of these materials with crystalline pore walls achieved by π-π stacking of aromatic bridging groups.[22–27] Beside a couple of works[28,29] suggesting a very limited molecular ordering in the pore walls of PMOs prepared under acidic conditions, the reported so far PMOs

* Corresponding author. Phone: 82-31-299 4707(D.K.) (330) 672 3790 (M.J.). E-mail: djkim@skku.edu (D.K.); jaroniec@kent.edu (M.J.).
† Sungkyunkwan University.
‡ Kent State University.

(1) Kresge, C. T.; Leonowicz, M. E.; Roth, W. J.; Vartuli, J. C.; Beck, J. S. *Nature* **1992**, *359*, 710–712.
(2) Yang, H.; Coombs, N.; Ozin, G. A. *Nature* **1997**, *386*, 692–695.
(3) Corma, A. *Chem. Rev.* **1997**, *97*, 2373–2420.
(4) Zhao, D.; Feng, J.; Huo, Q.; Melosh, N.; Fredrickson, G. H.; Chmelka, B. F.; Stucky, G. D. *Science* **1998**, *279*, 548–552.
(5) Ying, J. Y.; Mehnert, C. P.; Wong, M. S. *Angew. Chem., Int. Ed.* **1999**, *38*, 56–77.
(6) Soler-Illia, G. J. de A. A.; Sanchez, C.; Lebeau, B.; Patarin, J. *Chem. Rev.* **2002**, *102*, 4093–4138.
(7) Sanchez, C.; Soler-Illia, G. J. de A. A.; Ribbot, F.; Lalot, T.; Mayer, C. R.; Cabuil, V. *Chem. Mater.* **2001**, *13*, 3061–3083.
(8) Sayari, A.; Hamoudi, S. *Chem. Mater.* **2001**, *13*, 3151–3168.
(9) Hunks, W. J.; Ozin, G. A. *J. Mater. Chem.* **2005**, *15*, 3716–3724.
(10) Hoffman, F.; Cornelius, M.; Morell, J.; Fröba, M. *Angew. Chem., Int. Ed.* **2006**, *45*, 3216–3251.
(11) Schüth, F.; Schmidt, W. *Adv. Mater.* **2002**, *14*, 629–638.
(12) Stein, A. *Adv. Mater.* **2003**, *15*, 763–775.
(13) Yang, H.; Zhao, D. *J. Mater. Chem.* **2005**, *15*, 1217–1231.
(14) Xia, Y.; Yang, Z.; Mokaya, R. *Chem. Mater.* **2006**, *18*, 1141–1148.
(15) Xia, Y.; Mokaya, R. *J. Phys. Chem B* **2006**, *110*, 3889–3894.
(16) Asefa, T.; Yoshina-Ishii, C.; MacLaclan, M.; Ozin, G. A. *J. Mater. Chem.* **2000**, *10*, 1751–1755.
(17) Burleigh, M. C.; Markowitz, M. A.; Jayasundera, S.; Spector, M. S.; Thomas, C. W.; Gaber, B. P. *J. Phys. Chem B* **2003**, *107*, 12628–12634.
(18) Cho, E.-B.; Char, K. *Chem. Mater.* **2004**, *16*, 270–275.
(19) Vinu, A.; Hossain, K. Z.; Ariga, K. *J. Nanosci. Nanotechnol.* **2005**, *5*, 347–371.
(20) Hoffman, F.; Cornelius, M.; Morell, J.; Fröba, M. *J. Nanosci. Nanotechnol.* **2006**, *6*, 265–288.
(21) Jaroniec, M. *Nature* **2006**, *442*, 638–640.
(22) Inagaki, S.; Guan, S.; Ohsuna, T.; Terasaki, O. *Nature* **2002**, *416*, 304–307.
(23) Goto, Y.; Inagaki, S. *Chem. Commun.* **2002**, 2410–2411.
(24) Yang, Q.; Kapoor, M. P.; Inagaki, S. *J. Am. Chem. Soc.* **2002**, *124*, 9694–9695.
(25) Kapoor, M. P.; Inagaki, S.; Ikeda, S.; Kakiuchi, K.; Suda, M.; Shimada, T. *J. Am. Chem. Soc.* **2005**, *127*, 8174–8178.
(26) Sayari, A.; Wang, W. *J. Am. Chem. Soc.* **2005**, *127*, 12194–12195.
(27) Rebbin, V.; Schmidt, R.; Fröba, M. *Angew. Chem., Int. Ed.* **2006**, *45*, 5210–5214.
(28) Temtsin, G.; Asefa, T.; Bittner, S.; Ozin, G. A. *J. Mater. Chem.* **2001**, *12*, 3202–3206.
(29) Wang, W.; Zhou, W.; Sayari, A. *Chem. Mater.* **2003**, *15*, 4886–4889.

10.1021/cm702307s CCC: $40.75
Published on Web 03/13/2008

with truly crystalline walls were synthesized under basic conditions using cationic surfactants as templates.[22–27] In general, the most of PMOs prepared in the presence of high-molecular-weight nonionic surfactant templates under acidic conditions exhibits mesostructural ordering[30–35] but lacks the molecular-scale ordering even in the case of aromatic bridging groups. While the stacking of aromatic moieties occurs easily in PMOs templated by cationic surfactants under basic conditions, its presence in PMOs formed in the block copolymers phases under acidic conditions requires some additives as shown recently by Yang and Sayari.[36] For instance, n-butanol was added during synthesis of polymer-templated PMO with biphenyl bridges to obtain the crystalline pore walls under acidic conditions.[36] Thus, the synthesis of polymer-templated crystalline PMOs under acidic conditions is still a challenging task.

Another issue requiring attention in the study of PMOs is the pore size tailoring. There are only a few reports on the control of pore diameters in PMOs.[37,38] Usually, the chain length of ionic surfactants and the size of hydrophobic and hydrophilic segments of block copolymers have been used to tailor the pore size of mesoporous materials; however, inorganic salts have been mainly employed to control the particle morphology and to improve the pore size uniformity in mesoporous silica materials.[39–47] Also, sodium and potassium inorganic salts have been used to improve the structural ordering of PMOs.[47–52] However, there is only one publication[53] showing the improvement of the ethane-silica structure formed in the presence of divalent inorganic salts of Ni, Zn, and Mg and another anion (F^-)-containing salt under neutral conditions using oligomeric surfactant Brij-76 as a template. Since the divalent salts seem to be more effective for the improvement of surfactant-templated ethane-PMO structures, it would be interesting to study the effect of other inorganic salts on the formation of benzene-PMOs as well as ethane-PMOs and to take a full advantage of this effect for tailoring the physicochemical properties of these materials.

This work reports the effect of trivalent aluminum compounds on the synthesis of polymer-templated PMOs under acidic conditions. The synthesis of large pore ethane-PMOs and benzene-PMOs in the presence of aluminum chloride, sodium aluminate, and aluminum butoxide as aluminum sources was performed mainly by using a poly(ethylene oxide)-poly(DL-lactic acid-co-glycolic acid)-poly(ethylene oxide) (PEO-PLGA-PEO) triblock copolymer as template. The role of aluminum salts was manifested by promoting the formation of polymeric micelles and controlling pH of the synthesis gel, which affected the mesostructure ordering, pore volume, pore size, pore wall crystallinity, and particle morphology of PMOs with ethane and benzene bridging groups. In particular, a highly ordered 2D hexagonal benzene-silica mesostructure was synthesized by using a small amount of $AlCl_3$ (a strong Lewis acid) instead of HCl, as a new promoter mediating supramolecular interactions between PEO chains and BTEB precursor. Moreover, PEO-containing block copolymer templates of different hydrophobicity as well as inorganic salts of different ionic strength were used to tune interactions between PEO blocks and organosilica precursors, which are essential for the development of porosity in PMOs.

Experimental Section

Synthesis of Triblock Copolymers. Poly(ethylene oxide)-poly(DL-lactic acid-co-glycolic acid)-poly(ethylene oxide), EO_{16}-$(L_{29}G_7)EO_{16}$, triblock copolymer (denoted as LGE538) was synthesized through sequential reactions procedure using 50 g of DL-lactide (Aldrich), 10 g of glycolide (Polyscience), 40 g of monomethoxy poly(ethylene oxide) ($M_n = 750$ g mol^{-1}, Aldrich), 6.15 mL of stannous 2-ethyl hexanoate (Sigma), and 4.5 mL of hexamethylene diisocyanate (Sigma) in an appropriate quantity of anhydrous toluene solvent at 393 K under nitrogen atmosphere as reported elsewhere.[18] The final LGE538 triblock copolymer was obtained by successive filtration, evaporation of the solvent, and drying in a vacuum for 15 days, after precipitating the copolymer in cold diethyl ether several times. Poly(ethylene oxide)-poly(propylene oxide)-poly(ethylene oxide) P123 ($EO_{20}PO_{70}EO_{20}$, BASF) block copolymer was used as purchased.

The average molecular weight of LGE538 was determined to be 5,310, and the polydispersity index was 1.28 estimated by using a GPC-RI (Waters HPLC) system coupled with a Water 2410 differential refractive index detector. The flow rate of chloroform used as a mobile phase was 0.8 mL min^{-1}. Also, the ^{1}H NMR (500 MHz) spectrum was recorded on a Varian Unity Inova 500NB FT-NMR system using DMSO solvent at 373 K and used to estimate the molecular weight of the LGE538 polymer. The NMR data gave about 20% smaller value; namely, 4,220 Daltons. The volume fraction of the PEO blocks (Φ_{PEO}) was estimated to be 0.38; this estimation was performed by the group contribution

(30) Yoshina-Ishii, C.; Asefa, T.; Coombs, N.; MacLachlan, M. J.; Ozin, G. A. *Chem. Commun.* **1999**, 2539–2540.
(31) Inagaki, S.; Guan, S.; Fukushima, Y.; Ohsuna, T.; Terasaki, O. *J. Am. Chem. Soc.* **1999**, *121*, 9611–9614.
(32) Guan, S.; Inagaki, S.; Ohsuna, T.; Terasaki, O. *J. Am. Chem. Soc.* **2000**, *122*, 5660–5661.
(33) Kapoor, M. P.; Inagaki, S. *Chem. Mater.* **2002**, *14*, 3509–3514.
(34) Morell, J.; Woltner, G.; Fröba, M. *Chem. Mater.* **2005**, *17*, 804–808.
(35) Cho, E.-B.; Kim, D. *Chem. Lett.* **2007**, *36*, 118–119.
(36) Yang, Y.; Sayari, A. *Chem. Mater.* **2007**, *19*, 4117–4119.
(37) Hamoudi, S.; Yang, Y.; Moudrakovski, I. L.; Lang, S.; Sayari, A. *J. Phys. Chem. B* **2001**, *105*, 9118–9123.
(38) Bion, N.; Ferreira, P.; Valente, A.; Goncalves, I. S.; Rocha, J. *J. Mater. Chem.* **2003**, *13*, 1910–1913.
(39) Ryoo, R.; Jun, S. *J. Phys. Chem. B* **1997**, *101*, 317–320.
(40) Kim, J. M.; Jun, S.; Ryoo, R. *J. Phys. Chem. B* **1999**, *103*, 6200–6205.
(41) Schmidt-Winkel, P.; Yang, P.; Margolese, D. I.; Chmelka, B. F.; Stucky, G. D. *Adv. Mater.* **1999**, *11*, 303–307.
(42) Zhao, D.; Yang, P.; Chmelka, B. F.; Stucky, G. D. *Chem. Mater.* **1999**, *11*, 1174–1178.
(43) Prouzet, E.; Cot, F.; Nabias, G.; Larbot, A.; Kooyman, P.; Pinnavaia, T. J. *Chem. Mater.* **1999**, *11*, 1498–1503.
(44) Zhao, D.; Sun, J.; Li, Q.; Stucky, G. D. *Chem. Mater.* **2000**, *12*, 275–279.
(45) Yu, C.; Tian, B.; Fan, J.; Stucky, G. D.; Zhao, D. *Chem. Commun.* **2001**, 2726–2727.
(46) Yu, C.; Tian, B.; Fan, J.; Stucky, G. D.; Zhao, D. *J. Am. Chem. Soc.* **2002**, *124*, 4556–4557.
(47) Guo, W.; Park, J.-Y.; Oh, M.-O.; Jeong, H.-W.; Cho, W.-J.; Kim, I.; Ha, C.-S. *Chem. Mater.* **2003**, *15*, 2295–2298.
(48) Guo, W.; Kim, I.; Ha, C. S. *Chem. Commun.* **2003**, 2692–2693.
(49) Yang, Q.; Liu, J.; Yang, J.; Kapoor, M. P.; Inagaki, S.; Li, C. *J. Catal.* **2004**, *228*, 265–272.
(50) Zhao, L.; Zhu, G.; Zhang, D.; Di, Y.; Chen, Y.; Terasaki, O.; Qiu, S. *J. Phys. Chem. B* **2005**, *109*, 764–768.
(51) Landskron, K.; Ozin, G. A. *Science* **2004**, *306*, 1529–1532.
(52) Grudzien, R. M.; Grabicka, B. E.; Jaroniec, M. *Adsorption* **2006**, *12*, 293–308.
(53) Zhang, L.; Yang, Q.; Zhang, W.-H.; Li, Y.; Yang, J.; Jiang, D.; Zhu, G.; Li, C. *J. Mater. Chem.* **2005**, *15*, 2562–2568.
(54) Jaroniec, M.; Solovyov, L. A. *Langmuir* **2006**, *22*, 6757–6760.

Table 1. Physicochemical Properties of 2D Hexagonally Ordered Ethane-Silicas Prepared by Using PEO-PLGA-PEO Block Copolymer Template and Various Inorganic Compounds as Additives[a]

sample	inorganic additives	pH	[I]/[BTEE]	S_{BET} (m^2 g^{-1})	V_t (cm^3 g^{-1})	V_c (cm^3 g^{-1})	d_{100} (nm)	D_p (nm)	W (nm)	R_{Al} (ppm)
LES		0.35	0.0	897	1.23	0.12	10.5	8.62	3.50	N/A
LES_K	KCl	0.35	1.0	967	1.69	0.08	9.3	8.18	2.56	N/A
LES_C	$CaCl_2$	0.24	1.0	898	1.50	0.09	9.4	8.29	2.56	N/A
LES_A	$AlCl_3$	0.17	1.0	895	1.37	0.10	9.5	8.41	2.56	268.6
LES_NA	$NaAlO_2$	0.20	0.25	1072	1.72	0.10	9.8	9.27	2.05	80.65

[a] Notation: pH, measured after the addition of inorganic additives; [I]/[BTEE], molar ratio of inorganic additive to BTEE; S_{BET}, BET specific surface area determined in the range of relative pressures from 0.05 to 0.2; V_t, single-point pore volume; V_c, volume of complementary pores estimated by subtracting the mesopore volume obtained by integration of PSD above 3 nm from the single-point pore volume; D_p, mesopore diameter at the maximum of the PSD curve obtained by the improved KJS method;[54] W, pore wall thickness $= d_{100} \times 2/\sqrt{3} - D_p$; R_{Al}, residual aluminum content in final product.

Table 2. Physicochemical Properties of 2D Hexagonally Ordered Benzene-Silicas Prepared by using PEO-PLGA-PEO Block Copolymer Template and Various Inorganic Compounds as Additives[a]

sample	inorganic additives	pH	[I]/[BTEB]	S_{BET} (m^2 g^{-1})	V_t (cm^3 g^{-1})	V_c (cm^3 g^{-1})	d_{100} (nm)	D_p (nm)	W (nm)	R_{Al} (ppm)
LBS		1.39	0.0	982	0.99	0.22	9.7	8.43	2.77	N/A
LBS_K	KCl	1.22	1.0	1226	1.33	0.19	8.6	7.78	2.15	N/A
LBS_C	$CaCl_2$	1.13	1.0	1144	1.24	0.19	8.6	7.98	1.95	N/A
LBS_A	$AlCl_3$	0.86	1.0	1206	1.28	0.22	8.5	7.99	1.82	768.0
LBS_AA	$AlCl_3$	2.47	1.7	1131	1.27	0.19	9.3	8.24	2.50	5163
LBS_NA	$NaAlO_2$	1.16	0.25	842	0.91	0.16	9.5	8.03	2.94	2244
LBS_AB	$Al(O^sBu)_3$	1.27	0.25	730	0.80	0.12	9.4	8.19	2.67	2162

[a] Notation: pH, measured after the addition of inorganic additives; [I]/[BTEB], molar ratio of inorganic additive to BTEB; S_{BET}, BET specific surface area determined in the range of relative pressures from 0.05 to 0.2; V_t, single-point pore volume; V_c, volume of complementary pores estimated by subtracting the mesopore volume obtained by integration of PSD above 3 nm from the single-point pore volume; D_p, mesopore diameter at the maximum of the PSD curve obtained by the improved KJS method;[54] W, pore wall thickness $= d_{100} \times 2/\sqrt{3} - D_p$; R_{Al}, residual aluminum content in final product; LBS_AA, mesoporous benzene-silica sample was prepared without HCl.

method on the basis of the molar composition obtained by analysis of the NMR spectrum.

Preparation of Periodic Mesoporous Organosilicas. LGE538 triblock copolymer was used as a main template, and 1,2-bis(triethoxysilyl)ethane (BTEE, Aldrich) and 1,4-bis(triethoxysilyl)benzene (BTEB, Aldrich) were used as organo-bridged silica precursors. Aluminum chloride ($AlCl_3$, Aldrich) was used as a main inorganic salt, and potassium chloride (KCl, Aldrich) and calcium chloride ($CaCl_2$, Aldrich) were used as other inorganic sources. In addition, sodium aluminate ($NaAlO_2$, Strem) and aluminum butoxide ($Al(O^sBt)_3$, Strem) were used as the other aluminum-containing additives.

In a typical synthesis of ethane-PMO (e.g., LES_NA in Table 1), 0.5 g of LGE538 triblock copolymer was dissolved in a mixture of 19.28 g of distilled water and 1.0 g of ethanol, and after stirring the polymer solution for 1 h, 2.22 g of HCl (37 wt %, Aldrich) was added. After 2 h of additional stirring, the mixture of BTEE (0.720 g) and sodium aluminate (0.125 g) were added.

In a synthesis of benzene-PMO (e.g., LBS_AA in Table 2), 0.5 g of LGE538 triblock copolymer, 22.0 g of distilled water, 0.5 g of ethanol, 0.44 g of $AlCl_3$, and 0.80 g of BTEB were used. Precipitates were obtained by stirring the mixture at 313 K within 2 h for all samples studied except for the LBS_AA sample (within 12 h); finally all samples were subjected to aging for 24 h at 373 K. 60 g of acetone was used as a washing solvent under magnetic stirring for 5 h at 329 K to remove the block copolymer template and remaining inorganic materials. Finally, the product was washed with distilled water using a suction flask and dried at 373 K for 1 day.

Measurements and Calculations. The small-angle X-ray scattering experiments were performed using a Bruker SAXS analyzer having a 2D GADDS diffractometer and Cu Kα radiation with $\lambda = 1.54$ Å. The wide-angle X-ray measurements were performed using Bruker WAXS analyzer with a goniometer of 600 mm and a 2-dimensional area detector. The WAXS data were collected and taken by the CCD camera and converted to spectra versus 2θ from 5 to 40 degrees. The TEM images were obtained with an FE-TEM (JEOL JEM2100F) operated at an accelerating voltage of 200 kV. The samples were sonicated for 60 min in an adequate quantity of ethanol and the solution was dropped onto a porous carbon film on a copper grid and then dried. The SEM images were obtained with a field emission SEM (JEOL JSM6700F) operated at an accelerating voltage of 15 kV.

Nitrogen adsorption–desorption isotherms were measured on a Micromeritics 2020 analyzer. The samples were degassed at 423 K to achieve vacuum below 30 μmHg. The BET (Brunauer-Emmet-Teller) specific surface area was calculated from the adsorption data in the relative pressure range from 0.05 to 0.2. The total pore volume was evaluated from the amount adsorbed at a relative pressure of 0.99. The volume of complementary (fine) pores was estimated by subtracting the mesopore volume obtained by integration of pore size distribution (PSD) above 3 nm from the single-point pore volume. The PSD curves were calculated from the adsorption branches of the isotherms by using the improved KJS (Kruk-Jaroniec-Sayari) method.[54] The pore width was estimated at the maximum of PSD.

The solid-state NMR spectra were obtained with a Bruker DSX400 spectrometer using a 4 mm magic angle (MAS) spinning probe at the Korea Basic Science Institute. The samples analyzed by ^{29}Si MAS NMR were spun at a rate of 6 kHz and the chemical shifts were obtained with respect to the tetramethylsilane reference peak. The samples analyzed by ^{27}Al MAS NMR were spun at a rate of 13 kHz and the signals were referenced to a 1.0 M aqueous solution of aluminum chloride ($AlCl_3$). The ^{29}Si MAS NMR spectra were obtained with a recycle delay of 50 s and 2,000 scans; and the ^{27}Al MAS NMR spectra were recorded with a recycle delay of 1 s and 1000 scans. The structural quantification of the carbon-silicon linkages was performed through the simulation and decomposition of the ^{29}Si MAS NMR spectra. Residual aluminum contents were quantified with 138 Ultrace (Jobin Yvon) inductively coupled plasma-atomic emission spectroscopy (ICP-AES) using argon plasma of 6000 K at Korea Basic Science Institute.

Results and Discussion

Five ethane-PMOs samples were prepared in the presence of PEO-PLGA-PEO template by varying inorganic additives

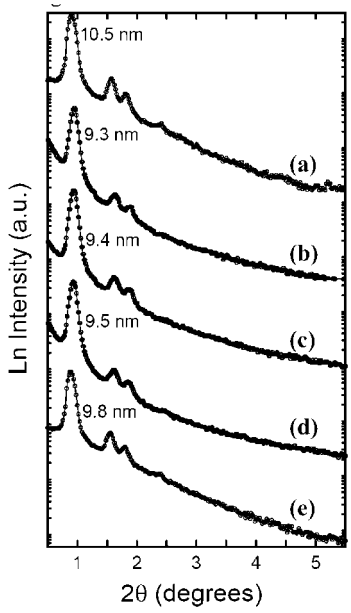

Figure 1. 2D SAXS patterns for ethane-PMOs prepared using LGE538 triblock copolymer, BTEE, and inorganic salts under strongly acidic conditions. The sample names and reactants correspond to the sequence of samples listed in Table 1: (a) without salt, (b) with KCl, (c) with $CaCl_2$, (d) with $AlCl_3$, and (e) with $NaAlO_2$, respectively.

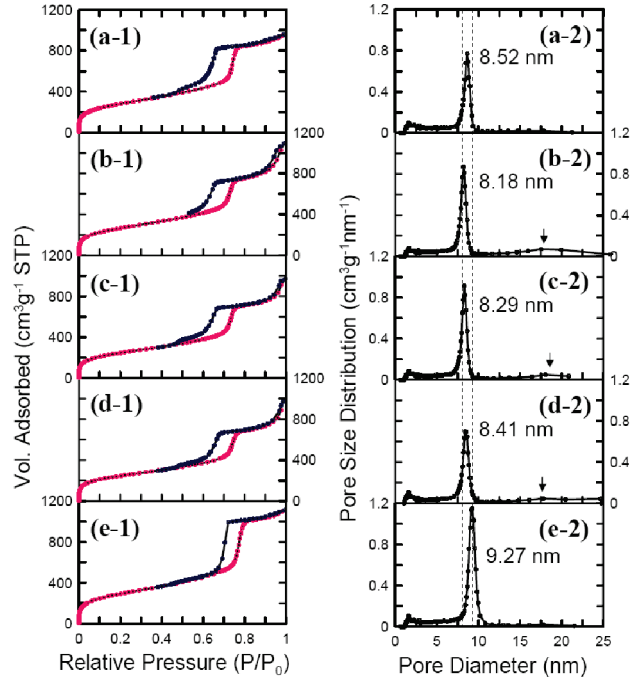

Figure 2. Nitrogen adsorption–desorption isotherms and the corresponding pore size distributions for ethane-PMOs prepared using LGE538 triblock copolymer, BTEE, and inorganic salts under strongly acidic conditions. The sample names and reactants correspond to the sequence of samples listed in Table 1: (a-1, a-2) without salt, (b-1, b-2) with KCl, (c-1, c-2) with $CaCl_2$, (d-1, d-2) with $AlCl_3$, and (e-1, e-2) with $NaAlO_2$, respectively.

under strong acidic conditions as shown in Table 1. The 2D SAXS results for ethane-PMO powder materials are shown in Figure 1. As can be seen from this figure all template-free ethane-PMOs are highly ordered 2D hexagonal (*p6mm*) mesostructures with at least three well-resolved peaks indexed as the (100), (110), and (200) reflections; however, LES prepared without salt and LES_NA prepared with sodium aluminate exhibit the fourth (210) reflection as shown in Figure 1a,e. The most intense Bragg peak shifts causing a decrease in the *d*-spacing from 10.5 to 9.3 nm with adding inorganic species and this shrinkage obeys the following order: KCl > $CaCl_2$ > $AlCl_3$. In this case inorganic additives acted as micellization-promoting (i.e., "salting-out") agents by increasing hydrophobicity of PEO blocks and lowering the thermodynamic radius of micelles, which led to a decrease in the cell parameter.[45] On the other hand, the acidity of synthesis mixture was reduced in the reverse order: $AlCl_3$ > $CaCl_2$ > KCl (Table 1), which corresponds to the acidity of the inorganic salts added. The formation of a well-defined 2D hexagonal (*p6mm*) structure of ethane-PMO was also confirmed by the TEM images shown in the Supporting Information, Figure S1.

The nitrogen adsorption–desorption isotherms for ethane-PMOs are type IV with a steep increase of adsorption branch at P/P_0 of about 0.70–0.80 due to the capillary condensation of nitrogen in the mesopores (Figure 2). The BET surface areas for this series of PMOs are in the range from 895 to 1072 $m^2\ g^{-1}$ and the total pore volumes are from 1.23 to 1.72 $cm^3\ g^{-1}$. They show the highest values when sodium aluminate is used as an auxiliary agent. The relative ratios of the volume of complementary pores to the total pore volume decrease from 6.8 to 4.7% and LES_K sample shows the lowest value, which suggests a small suppression of the formation of these pores by adding KCl. The pore size distributions obtained from the adsorption isotherms by the improved KJS method[54] are narrow indicating high uniformity of porous structures (Figure 2). The pore diameters estimated at the maximum of the PSD curves are in the range from 8.18 to 9.27 nm; consequently, the pore wall thicknesses decrease from 3.50 to 2.05 nm. Analysis of adsorption and structural parameters listed in Table 1 and Figure 2 shows that the addition of sodium aluminate caused an increase in the specific surface area, the pore volume, the pore diameter as well as improved the quality of adsorption–desorption hysteresis of the ethane-silica samples studied, while the addition of KCl, $CaCl_2$, and $AlCl_3$ caused a decrease in the pore diameter and the relative amount of complementary pores. In addition, these salts promoted the formation of textural (secondary) mesoporosity as evidenced by small portion of pores above 15 nm shown in Figure 2(b-2, c-2, d-2), which may be an indication that inorganic salts are able to enhance the intermicellar aggregation in comparison to the formation of ordered BTEE-PEO interface. As shown in Table 1 and Figures 1 and 2 the addition of the aforementioned inorganic salts can be used to tailor to some extent the adsorption and structural properties of ethane-silicas. The role of these inorganic salts can be explained in terms of balancing the hydrophobicity/hydrophilicity and micellization of block copolymers, which are essential for self-assembly process in an aqueous solution.

Solid-state ^{29}Si NMR measurements for ethane-PMOs were performed to verify the composition and structure of the covalently bonded ethane-bridging groups in the PMO framework. The characteristic signals on the ^{29}Si MAS NMR spectra of ethane-PMOs (Supporting Information Figures S2) are assigned to C-*Si*$(OSi)_3$ (T^3, $\delta = -65$ ppm), C-*Si*-

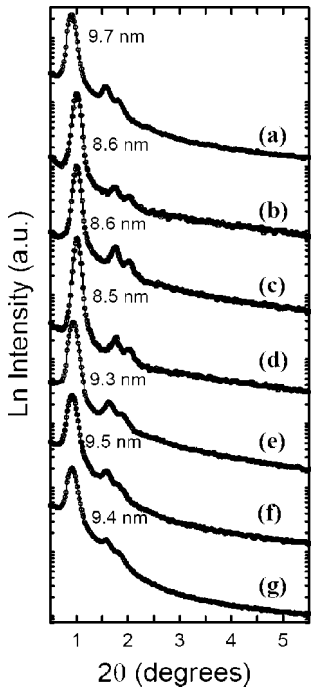

Figure 3. 2D SAXS patterns for benzene-PMOs prepared using LGE538 triblock copolymers, BTEB, and inorganic salts under acidic conditions. The sample names and reactants correspond to the sequence of samples listed in Table 2: (a) without salt, (b) with KCl, (c) with $CaCl_2$, (d) with $AlCl_3$, (e) with $AlCl_3$ but without HCl, (f) with $NaAlO_2$, and (g) with $Al(O^sBu)_3$, respectively.

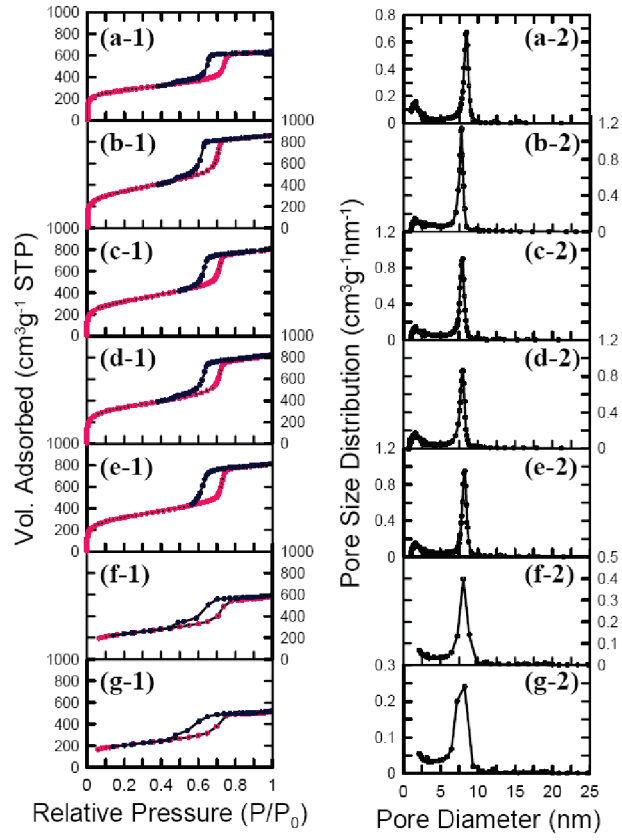

Figure 4. Nitrogen adsorption–desorption isotherms and the corresponding pore size distributions for benzene-PMOs prepared using LGE538 triblock copolymer, BTEB, and inorganic salts under acidic conditions. The sample names and reactants correspond to the sequence of samples listed in Table 2: (a) without salt, (b) with KCl, (c) with $CaCl_2$, (d) with $AlCl_3$, (e) with $AlCl_3$ but without HCl, (f) with $NaAlO_2$, and (g) with $Al(O^sBu)_3$, respectively.

$(OSi)_2(OH)$ (T^2, $\delta = -57$ ppm), and C-*Si*$(OSi)(OH)_2$ (T^1, $\delta = -50$ ppm), respectively, which represent possible structures of Si species covalently bonded to carbon atoms. The relative amounts of $T^2 + T^3$ vary from 95.1 to 98.4%, and the T^3/T^2 ratio changes from 1.77 to 1.01, respectively; these quantities were estimated by simulation, deconvolution, and integration of the spectra as shown in the Supporting Information, Figure S2. However, there is a negligible resonance present on the ^{27}Al NMR spectrum recorded for the LES_A and LES_NA ethane-PMO (see the Supporting Information, Figure S3), which suggests that aluminum was not incorporated into PMO and aluminum chloride and sodium aluminate played the role of auxiliary salts that facilitated the structure formation of the resulting PMOs. A similar tendency was also observed when aluminum butoxide was used as aluminum source. The relatively small contents of residual aluminum were also determined by ICP-AES technique (Table 1).

Benzene-PMOs were prepared using BTEB precursor and LGE538 triblock copolymer template by varying inorganic additives under acidic conditions as shown in Table 2. The 2D SAXS spectra of benzene-PMOs prepared with inorganic additives are shown in Figure 3. As can be seen from this figure, all benzene-PMOs are highly ordered 2D-hexagonal (*p6mm*) mesostructures with at least three well-resolved peaks indexed as the (100), (110), and (200). The most intense Bragg peak shifts causing a decrease in the *d*-spacing from 9.7 to 8.5 nm with adding inorganic species and the shrinkage ("salting-out") effect is analogous for all the additives studied. The acidity of synthesis gels shows the same tendency as in the case of ethane-PMOs (i.e., $AlCl_3 > CaCl_2 > KCl$; Table 2). Especially, a highly ordered 2D hexagonal LBS_AA sample with large unit cell (10.7 nm), as shown in Figure 3e, was obtained by using aluminum chloride without HCl addition. Also, note that the second and third order peaks on the SAXS spectra of LBS_NA (Figure 3f) and LBS_AB (Figure 3g) prepared with sodium aluminate and aluminum butoxide, respectively, appear to have lower intensity in comparison to those for other benzene-PMOs and the LES_NA samples.

The nitrogen adsorption–desorption isotherms for benzene-PMOs are type IV with a steep increase of the adsorption branch at P/P_0 at about 0.65–0.80 (Figure 4). The BET surface areas for this series of PMOs are in the range from 730 to 1226 $m^2\ g^{-1}$ and the total pore volumes vary from 0.80 to 1.33 $cm^3\ g^{-1}$. They show the highest values when potassium chloride is used as an auxiliary compound. The relative ratios of the volume of complementary pores to the total pore volume decrease from 19.3 to 14.3% and LBS_K sample shows the lowest value, which is a similar as in the case of ethane-PMOs. The pore size distributions obtained from the adsorption isotherms by the improved KJS method[54] are very narrow indicating a high uniformity of porous structures (Figure 4). The pore diameters estimated at the maximum of PSD curves are in the range from 7.78 to 8.43 nm; consequently, the pore wall thicknesses vary from 2.94 to 1.82 nm. Analysis of adsorption and structural parameters

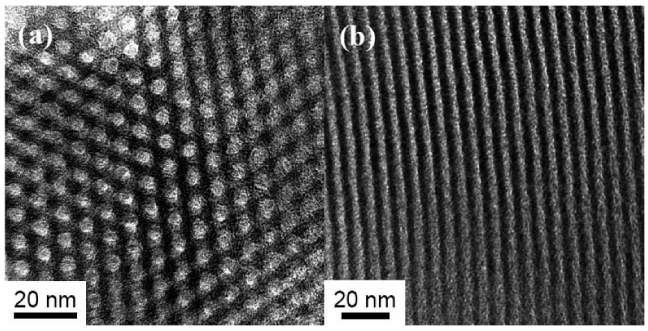

Figure 5. Representative TEM images for benzene-PMO prepared using LGE538 triblock copolymer, BTEB, and aluminum chloride without HCl addition.

listed in Table 2 and Figure 4 shows that KCl, $CaCl_2$, and $AlCl_3$ used caused an increase in the BET surface area and pore volume, and a decrease in the pore diameter, the wall thickness, and the relative amount of complementary pores. It is noteworthy that LBS_AA has a high BET surface area of 1131 $m^2\ g^{-1}$ and the pore volume of 1.27 $cm^3\ g^{-1}$ as well as a large pore diameter of 8.24 nm and narrow pore size distribution (Table 2 and Figure 4(e-1, e-2)). The formation of a well-defined 2D hexagonal (*p6mm*) structure of LBS_AA benzene-PMO was also confirmed by the TEM images shown in Figure 5. The surface areas of the LBS_NA (Figure 4f) and LBS_AB (Figure 4g) samples prepared with sodium aluminate and aluminum butoxide, respectively, are not so high in comparison to those of other benzene-PMOs (Table 2), which differentiates this series from that of LES_NA samples.

Benzene-silica samples were also prepared in the presence of LGE538 nonionic block copolymer template and inorganic compounds listed in Table 2 but without HCl addition. The 2D SAXS spectra for these benzene-PMO samples are shown in Figure 6. As can be seen from this figure all template-free benzene-silicas are not ordered structures except that shown in Figure 6d. The inorganic salts used were KCl, $CaCl_2$, $AlCl_3$, $NaAlO_2$, and $Al(O^sBu)_3$. The molar ratios of inorganic salt to BTEB were the same (i.e., [I]/[BTEB] = 1.7) for all the samples except that for the sample shown in Figure 6d ([I]/[BTEB] = 1). Note that the sample shown in Figure 6c was prepared using Pluronic P123 triblock copolymer template and the same molar quantity of aluminum chloride as that for the LBS_AA sample. Figure 6d exhibits three well-resolved peaks indexed as the (100), (110), and (200) reflections. The SAXS patterns in Figure 6 for the aforementioned benzene-PMO samples demonstrate clearly that among the additives studied the aluminum chloride with trivalent cation seems to be a more effective agent for the preparation of highly ordered benzene-PMO materials than other mono and divalent salts. Moreover, PEO-PLGA-PEO triblock copolymer is more effective template in comparison to the relatively hydrophilic PEO-PPO-PEO block copolymer for the synthesis of benzene-PMO when aluminum chloride is used without HCl addition. Also, it is noteworthy that the benzene-silica samples prepared with sodium aluminate and aluminum butoxide, as shown in Figure 6e,f, do not give Bragg peaks, which indicates that a strong anion such as chloride as well as an effective cation

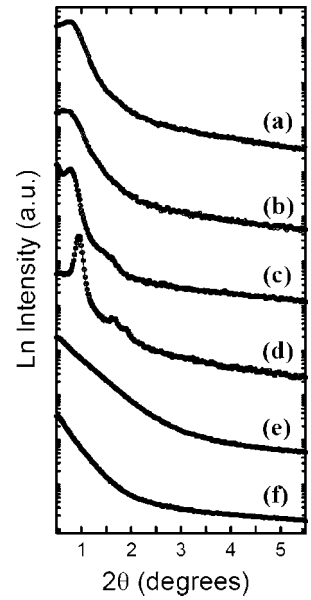

Figure 6. 2D SAXS patterns for benzene-PMOs prepared using LGE538 triblock copolymer, BTEB, and inorganic salts but without HCl addition. Inorganic salts used were (a) KCl, (b) $CaCl_2$, (c) $AlCl_3$, (d) $AlCl_3$, (e) $NaAlO_2$, and (f) $Al(O^sBu)_3$. The molar ratios ([I]/[BTEB]) for all the samples are the same (1.7) except that for the sample (d), which is 1.0. Sample (c) was prepared by using P123 triblock copolymer as a template.

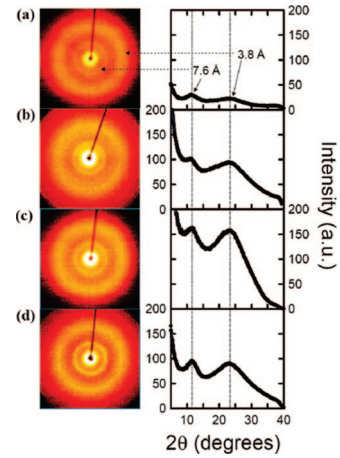

Figure 7. 2D WAXS images and the corresponding diffraction patterns for benzene-PMOs prepared using LGE538 triblock copolymer and BTEB under acidic conditions. Samples correspond to (a) LBS, (b) LBS_AA, (c) LBS_NA, and (d) LBS_AB labeled in Table 2, respectively.

are necessary to enhance interactions between PEO blocks and ethoxy-containing organosilica precursors.

The WAXS patterns together with two-dimensional images of benzene-PMOs shown in Figure 7 indicate the structural ordering of the pore walls of these materials. The 2D WAXS images, especially those on the left panels c and d in Figure 7, display two discrete rings corresponding to *d*-spacings of 0.76 and 0.38 nm, though the intensity is not so sharp to interpret it as a perfect crystalline phase. They are assigned to a periodic arrangement of benzene bridges within pore walls.[22] The diffraction patterns and intensities of the WAXS peaks for the benzene-PMOs prepared with addition of sodium aluminate and aluminum butoxide are higher than those for the corresponding samples with other inorganic salts or without salt addition, which is contrary to the intensity of long-range order peaks observed on the SAXS patterns

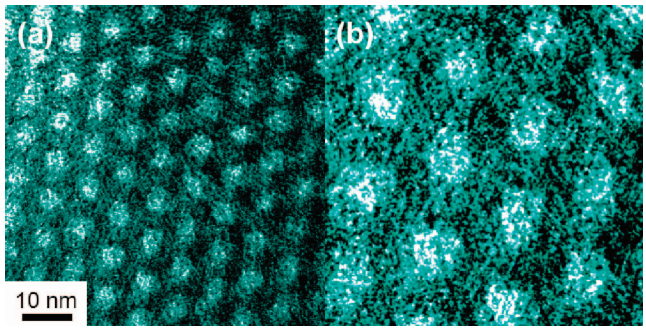

Figure 8. Representative TEM images for benzene-PMO prepared using LGE538 triblock copolymer, BTEB, and aluminum butoxide. Image (b) represents a magnified portion of (a).

(Figure 3f,g). The SAXS and WAXS patterns shown in Figures 3 and 7 indicate that sodium aluminate and aluminum butoxide cause an increase in the $\pi-\pi$ interactions between benzene moieties within the pore walls.

The FE-SEM images shown in the Supporting Information, Figure S4, present the morphology of the benzene-PMO synthesized using P123 triblock copolymer and sodium aluminate. The morphology of benzene-PMO prepared without salt addition is ropelike as reported elsewhere;[23] however, the morphology of benzene-PMOs prepared in this study exhibit a similar shape but with much higher aspect ratios (Supporting Information, Figure S4). Moreover, the surface of benzene-PMO rods has a multilayer structure. In contrast, the benzene-PMOs prepared by using the LGE538 triblock copolymer and sodium aluminate are in the form of spheres linked to each other.

Figure 8 shows a high resolution TEM image for benzene-PMO formed in the presence of the nonionic LGE538 triblock copolymer and aluminum butoxide. The image is perpendicular to the channel and represents a 2D hexagonally ordered mesostructure. As can be seen from this image the pore walls possess both amorphous and crystalline domains, which is consistent with the diffraction peaks obtained by wide-angle XRD. The aforementioned domains are shown more clearly in the magnified image of Figure 8b.

Solid-state ^{29}Si MAS NMR measurements for the polymer-free benzene-PMOs were performed to verify the composition and structure of the covalently bonded benzene-bridging groups in the pore walls. The ^{29}Si MAS NMR spectra for benzene-PMOs are shown in the Supporting Information, Figure S5. The characteristic signals observed on the ^{29}Si MAS NMR spectra of benzene-silicas are assigned to C-*Si*(OSi)$_3$ (T^3, $\delta = -78$), C-*Si*(OSi)$_2$(OH) (T^2, $\delta = -69$), and C-*Si*(OSi)(OH)$_2$ (T^1, $\delta = -61$), respectively, which reflect the structure of the Si species covalently bonded to the carbon atoms. The Q peaks such as *Si*(OSi)$_4$ and *Si*(OSi)$_3$(OH) were not observed between -90 and -120 ppm, which confirms that the cleavage of the C-Si bonds of the BTEB precursors did not occur during the sol–gel synthesis or the postsynthesis treatment steps. The relative amounts of $T^2 + T^3$ vary from 84.3 to 79.3%, and the T^3/T^2 ratio changes from 0.32 to 0.62, respectively. LBS_NA gives the highest value of the T^3/T^2 ratio; these quantities were estimated by simulation, deconvolution, and integration of the spectra as shown in the Supporting Information, Figure S5. The aforementioned values are not so high compared to those observed for mesoporous benzene-silica prepared using nonionic P123 triblock copolymer without addition of inorganic salts.[23]

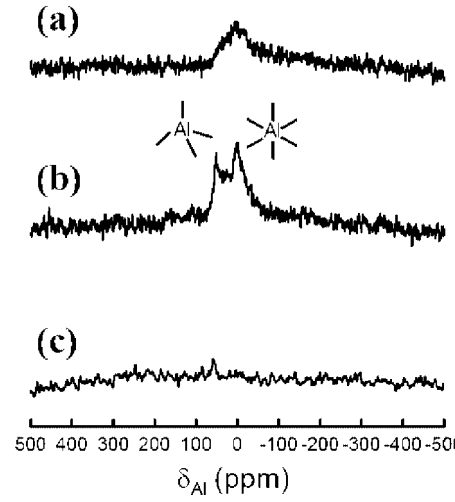

Figure 9. Representative solid state ^{27}Al MAS NMR spectra for benzene-PMOs studied; (a) LBS_A, (b) LBS_AA, and (c) LBS_NA correspond to the samples in Table 2.

Similarly to the ethane-PMO samples, the ^{27}Al NMR spectra for LBA_A and LBA_NA benzene-PMOs do not show meaningful resonances characteristic for aluminum species (Figure 9a, c), which indicates the absence of Al in the PMO framework. However, the ^{27}Al NMR spectrum for LBA_AA sample shows two weak resonances, which correspond to 4-fold (~60 ppm) and 6-fold (~1 ppm) coordinate aluminum, respectively, as shown in Figure 9b. Aluminum content in the LBA_AA sample estimated by ICP-AES was about 5 mg/g.

Conclusions

This study shows that trivalent aluminum salts affect differently the formation of polymer-templated PMOs with ethane and benzene bridging groups. Ethane-PMO (LEA_NA) prepared in the presence of sodium aluminate and PEO-PLGA-PEO triblock copolymer shows a high surface area, large pore volume, and pore diameter as well as a well-developed hysteresis loop without a two-step desorption branch. The effect of the remaining additives studied on the properties of ethane-silicas is less pronounced.

In the case of benzene-PMO, its adsorption properties were not much altered upon addition of sodium aluminate except for the increase of wall crystallinity. However, the addition of KCl, $CaCl_2$, and $AlCl_3$ caused an increase in the BET surface area and the pore volume, and a decrease in the pore diameter and the wall thickness. Especially, a highly ordered 2D hexagonal mesostructure was obtained for the PEO-PLGA-PEO triblock copolymer template in the presence of aluminum chloride but without HCl addition. It seems that the ordered mesostructure of benzene-silica could be prepared in the presence of aluminum chloride only (without HCl addition) because of enhanced formation of PEO-PLGA-PEO triblock copolymer micelles due to higher hydrophobicity

of this polymer. Moreover, the salt addition was essential for the structural ordering of benzene rings inside the pore walls, which is difficult to achieve under typical acidic conditions.

The present study shows clearly that inorganic salts affect the pH and micellization, which induces some porosity changes. Especially, aluminum chloride is more effective in lowering pH and increasing interactions between PEO blocks and BTEB, which facilitate the mesostructure formation. However, the addition of sodium aluminate and aluminum butoxide improves porosity of ethane-PMO and the wall crystallinity of benzene-PMO, respectively, which shows a great potential for tailoring PMOs by using adequate combinations of inorganic additives and block copolymer templates.

Acknowledgment. This work was partially supported by a Korea Research Foundation Grant (KRF 2006-005-J04601) and a Korean Science and Engineering Foundation (KOSEF) Grant funded by the Korea government (R0A-2007-000-10029-0). M.J. acknowledges support by the National Science Foundation under Grant CTS-0553014. Graduate students, Joanna Gorka and Pasquale Fulvio, from Kent State are acknowledged for help in adsorption measurements of several PMO samples.

Supporting Information Available: Three figures showing TEM images, ^{29}Si and ^{27}Al MAS NMR spectra for ethane-PMOs and two figures showing SEM images and ^{29}Si MAS NMR spectra for benzene-PMO samples (PDF). This material is available free of charge via the Internet at http://pubs.acs.org.

CM702307S